Prediction of wheel wear using Hertzian and non-Hertzian contact models

F. Alves[1], H. Magalhães[1], J. Pagaimo[1], J.N. Costa[1], F. Marques[2,3], J. Pombo[4,1,5], J. Ambrósio[1]

[1]IDMEC, Instituto Superior Técnico, Universidade de Lisboa, Lisboa, Portugal
[2]CMEMS-UMinho, Departamento de Engenharia Mecânica, Universidade do Minho, Guimarães, Portugal
[3]LABBELS – Associate Laboratory, Braga/Guimarães, Portugal
[4]Institute of Railway Research, School of Computing and Engineering, University of Huddersfield, Huddersfield, UK
[5]ISEL, Instituto Politécnico de Lisboa, Lisboa, Portugal

Abstract

Railway vehicles are periodically immobilized for wheel replacement or reprofiling once they reach the wear limits established by standards. Enhancing wheel designs and operating conditions may reduce wheel wear, saving high maintenance costs. Multibody simulations are useful to predict wheel wear evolution because they allow comparing different wheel-rail contact models. In this context, this work describes in detail a wear prediction tool that addresses parameters that the current literature often omits. The wear prediction tool is used to perform wheel wear analysis where both Hertzian and non-Hertzian contact models are utilised and compared to each other, contributing to the small literature body covering non-Hertzian contact model and wear prediction.

Keywords: Wear Prediction, Wheel-Rail Contact, Non-Hertzian contact, Multibody Dynamics.

1   Introduction

Railway transportation promotes an efficient, environmentally friendly, safe, and sustainable transportation network. Thus, improving dynamic performance and reducing associated costs is critical. In that sense, the study and prediction of wheel

wear in the context of multibody dynamics simulations is fundamental to enhancing the wheel design and controlling maintenance operations. The vehicles are periodically immobilized for inspection, reprofiling, and replacement of wheels due to their degradation, mainly caused by surface wear.

The prediction of wear involves predicting the lost or displaced volume of material from the contacting surfaces, which is a highly complex problem since it depends on several factors, namely, the geometry of the surfaces, sliding velocity, contact pressure, friction conditions, material characteristics, humidity, temperature, and presence of debris [1], [2]. These features influence the shape of the contact patch and the size of the adhesion and slippage regions, which ultimately affect the wear of profiles.

The relevance of this phenomenon led to the development of several computational methodologies to predict wear in wheel-rail contact using multibody simulation of railway vehicles. Although several authors have studied the wear evolution of wheel and rail profiles, the most popular wear models are the Archard, BRR, and USFD [3]. Regarding contact, most of the studies assume a simplified Hertzian contact combined with the FASTSIM algorithm to evaluate the tangential tractions. Thus, few works consider non-Hertzian contact models to predict wear progression during dynamic simulations [4], [5]. Since the vehicle must travel thousands of kilometres to achieve a substantial wear volume, assessing wear evolution requires simulations with long tracks and, therefore, computational efficiency is essential.

This work presents a wear prediction tool valid for Hertzian and non-Hertzian contact models [6]–[9]. The focus of this study is on the description of the numerical methods applied for the wear assessment, namely, to compute the wear, define the wear distribution or smooth the profiles, making this work replicable. The developed wear tool is demonstrated in an in-house multibody software, MUBODyn. The remainder of this work is organized as follows. Section 2 describes the methodology involved in the wear prediction tool. Section 3 applies the developed methods to a vehicle negotiating a curved track. Finally, section 4 presents the main conclusions of this work.

2   Methods

This section describes the wear prediction tool developed in this work that controls the multibody simulations performed in MUBODyn and post-processes their results according to the procedure schematized in Figure 1.

The wear is measured through the wear index $T\gamma$ defined by British Rail Research (BRR) wear model [3] which quantifies the energy dissipated during the wheel-rail contact through the work done by the creep forces. The BRR wear model is a global method, hence, it requires the global creep forces instead of tangential tractions distribution. This model defines three wear regimes that are associated with the magnitude of wear index, which is used to determine the area of material loss per rolled distance (Figure 2a). The area of loss material, A_{BRR}, is used to determine the wear depth of the main point of contact (Figure 2b), as

$$H_{\mathrm{BRR}} = \frac{D_i}{2} - \sqrt{\frac{D_i^2}{4} - \frac{A_{\mathrm{BRR}}}{\pi}}$$

(1)

where D_i denotes the wheel diameter at the corresponding lateral position. In the case of the Hertzian contact, the depth of wear over the contact patch can be estimated assuming an elliptical distribution as

$$H_{\mathrm{Hz}}(x, y) = H_{\mathrm{BRR}} \sqrt{1 - \frac{x^2}{a^2} - \frac{y^2}{b^2}}$$

(2)

in which a and b and the semi-axes of the contact area in the longitudinal and lateral directions, respectively. Regarding the non-Hertzian contact, a semi-Hertzian contact model is considered, therefore, an elliptical pressure distribution is established in the longitudinal direction. Moreover, it is proposed that the pressure distribution in the lateral direction is utilized to weigh the wear depth. Thus,

$$H_{\mathrm{nHz}}(x, y) = H_{\mathrm{BRR}} \frac{p_{\mathrm{n}}(0, y)}{p_0} \sqrt{1 - \frac{x^2}{x_{\mathrm{L}}(y)^2}}$$

(3)

where p_0 is the maximum normal pressure, $p_{\mathrm{n}}(0,y)$ represents the normal pressure along the contact patch lateral axis, and $x_{\mathrm{L}}(y)$ denotes the coordinate of the leading edge of the contact patch along the lateral direction.
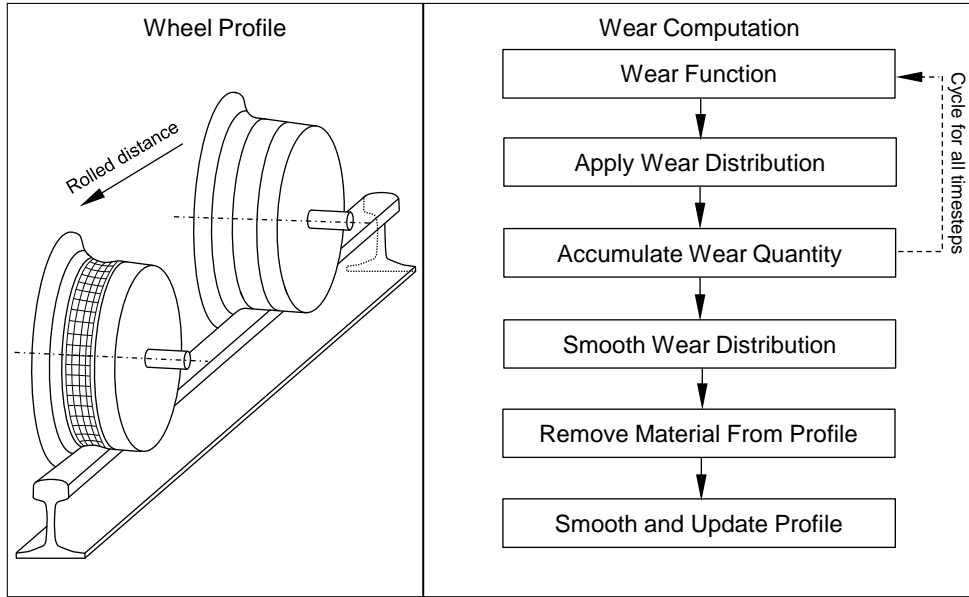

Figure 1: Wear prediction procedure.

To accumulate the wear, the profile is treated as a series of nodal points in which the wear will be added. One approach is applying the wear in the radial direction, however, this is not correct mainly when contact occurs on the flange or on the transition zone where the profile is far from horizontal. Thus, the wear depth is measured normal to the surface (Figure 3b).
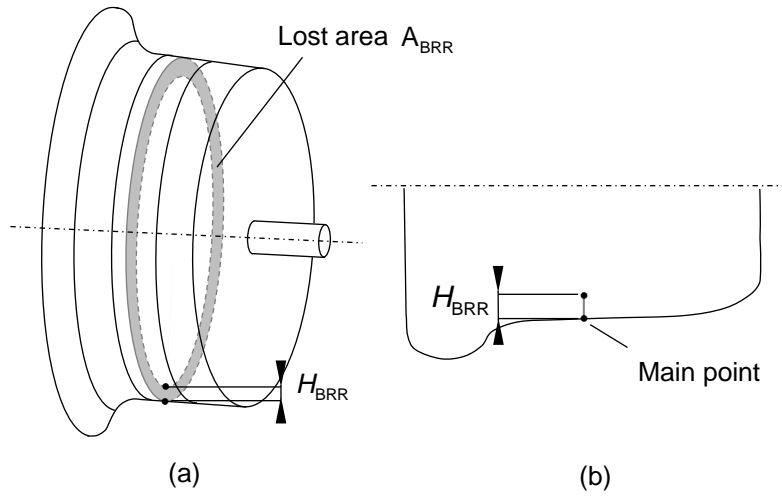
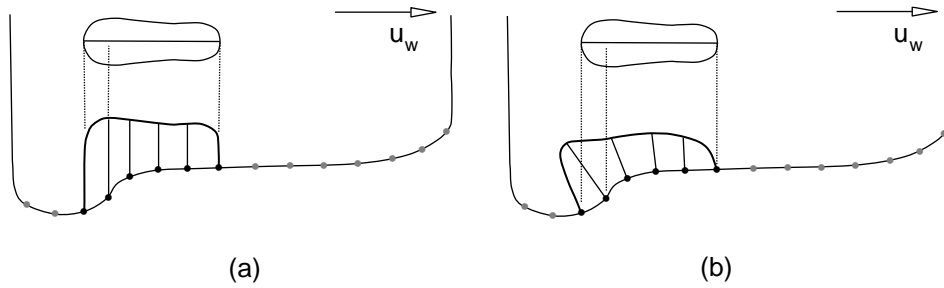Figure 2: (a) Removed area and (b) the correspondent wear depth H_{BRR}.

Figure 3: (a) Radial and (b) normal wear distribution.

In the end of a simulation, an array with the accumulated wear along the profile is obtained. Then, a moving average filter is applied to smooth the wear distribution and remove short wavelength concavities that have no physical meaning. The wheel profile is updated considering the obtained wear depth, which is scaled representing an artificial amplification of the running distance.

3   Results

The wear prediction tool described in the previous section is assessed through its application in a case scenario. The passenger vehicle proposed in the Manchester Benchmark is utilized in this study. The wheels have a nominal diameter of 920 mm, with the worn S1002 profile after 300,000 km, as represented in Figure 4. For this application case, the vehicle negotiates a right curve with a prescribed speed of 100 km/h, whose track layout parameters are presented in Figure 5. Track irregularities are included to obtain more realistic contact simulations, and the track flexibility is considered through a co-running model, which consist of having a model of rails, sleepers and foundation under each wheelset. The rails have the UIC60 profile with an inclination of 1/40, and the track gauge is 1435 mm.
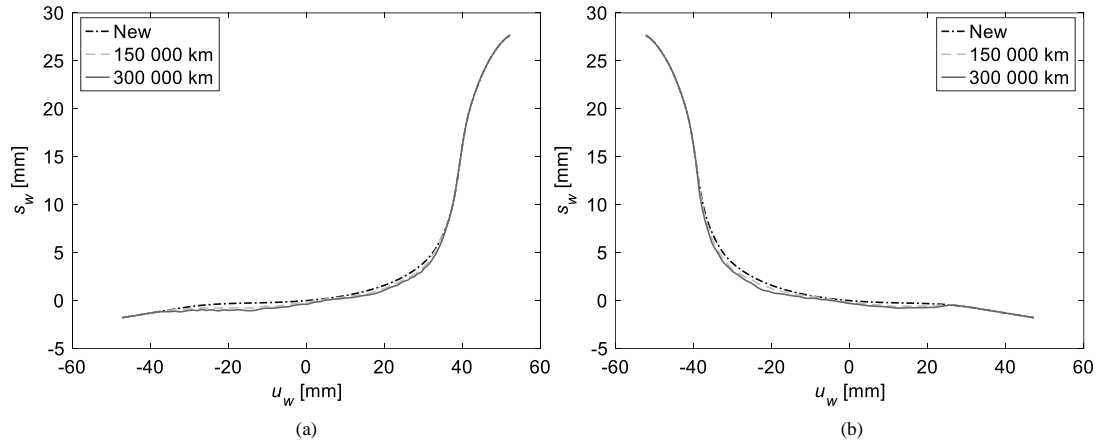
Figure 4: Evolution of worn wheel profiles of the leading wheelset for (a) left and (b) right sides.
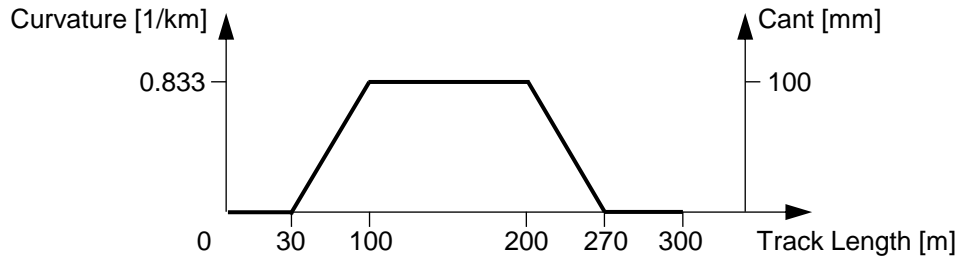

Figure 5: Curvature and cant of the track.

The simulation results are analyzed for the leading wheelset of the. Figure 6 shows location of the main points of contact on the wheel lateral direction along the track position for both Hertzian and non-Hertzian approaches. The results demonstrate that, in a worn profile, the contact tends to occur in specific locations due to the irregularities of the profile, with an overall agreement between both methods. These results also show that the contact patches obtained for both models in 25-meter intervals along the track. There is a strong tendency to have more than one contact patch at the same time, and both models present similar patches mainly in tread contact.

The resulting wear depth distribution obtained with the developed wear prediction tool is presented in Figure 7 for both left and right wheels. These results show that the Hertzian approach underestimates the wear volume when compared with non-Hertzian methodology. These differences are more prominent in the flange region, as shown in Figure 7a, which agrees with the fact that the contact patches tend to have a more non-elliptical shape in that region.
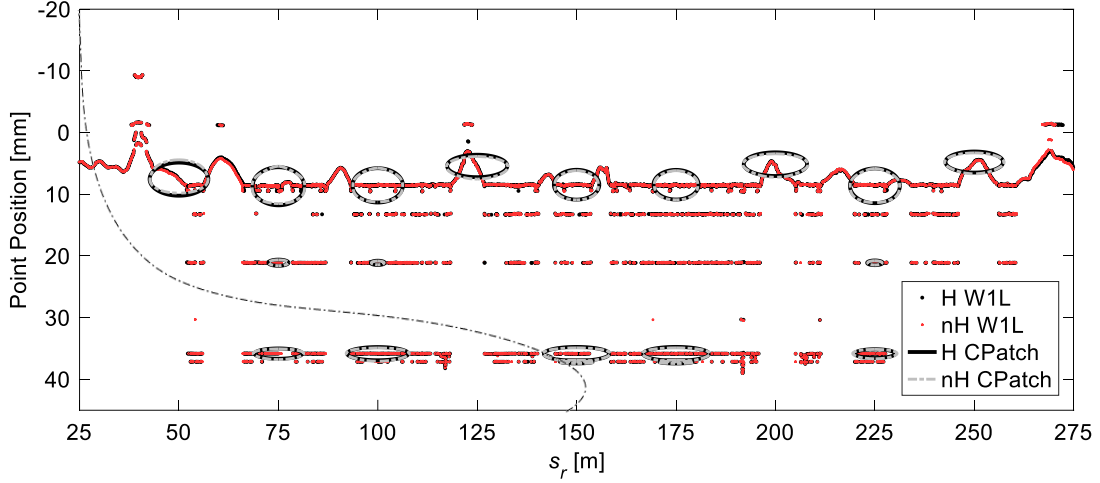
5

Figure 6: Location of the point of contact on the profile and some contact patches of the left leading wheel, for Hertzian and non-Hertzian contact models.
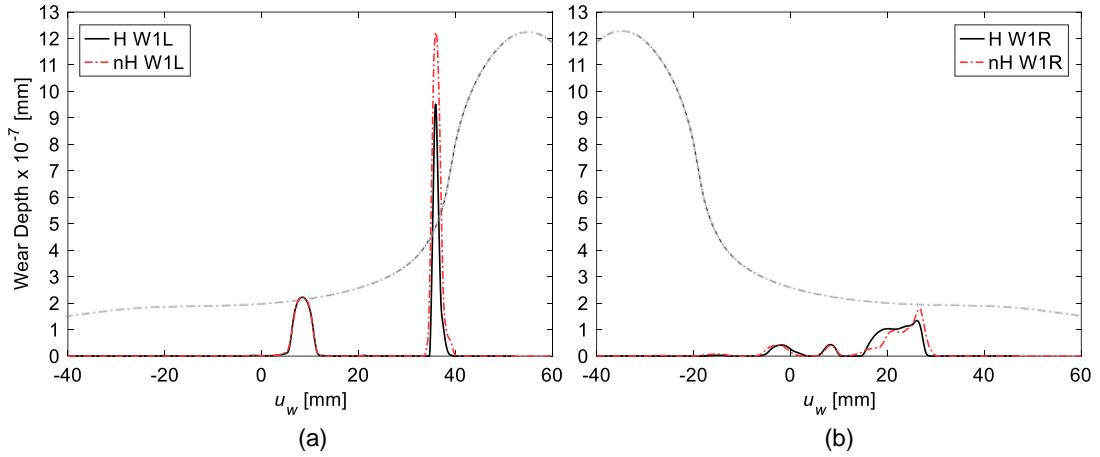

Figure 7: Wear depth comparison for (a) left and (b) right leading wheels, for both. Hertzian and non-Hertzian models. Dash dot line represents the wheel profile.

4   Conclusions and Contributions

This work presents a novel wear prediction tool valid for Hertzian and non-Hertzian contact models. This tool considers a wear depth distribution proportional to the normal pressure along the patch lateral direction. Moreover, the material is removed according to the surface normal direction, and the profile is smoothed to avoid short wavelength concavities while conserving the volume loss. These methodologies focus on the numerical aspects of this prediction tool, since they are not fully covered in the literature and although essential to ensure the correct implementation and its reproducibility. Furthermore, this method is demonstrated with an application example in which a vehicle runs on a flexible track comprising a right-hand curve and track irregularities. The results show significant differences between the amount of wear estimated by the Hertzian and non-Hertzian contact models.

6

The influence of some parameters of the proposed numerical methods, such as the profile refinement, direction of removed material, or smoothing length, will be studied in future work. More complex running scenarios will also be analyzed.

Acknowledgements

References

[1] R. Enblom, "Deterioration mechanisms in the wheel–rail interface with focus on wear prediction: a literature review," *Veh. Syst. Dyn.*, vol. 47, no. 6, pp. 661–700, 2009, doi: 10.1080/00423110802331559.

[2] B. Dirks and R. Enblom, "Prediction model for wheel profile wear and rolling contact fatigue," *Wear*, vol. 271, no. 1–2, pp. 210–217, 2011, doi: http://dx.doi.org/10.1016/j.wear.2010.10.028.

[3] J. Pombo *et al.*, "Development of a Wear Prediction Tool for Steel Railway Wheels Using Three Alternative Wear Functions," *Wear*, vol. 271, no. 1–2, pp. 238–245, 2011, doi: 10.1016/j.wear.2010.10.072.

[4] Y. Ye, Y. Sun, D. Shi, B. Peng, and M. Hecht, "A wheel wear prediction model of non-Hertzian wheel-rail contact considering wheelset yaw: Comparison between simulated and field test results," *Wear*, vol. 474–475, no. January, p. 203715, Jun. 2021, doi: 10.1016/j.wear.2021.203715.

[5] B. Zhu, J. Zeng, D. Zhang, and Y. Wu, "A non-Hertzian wheel-rail contact model considering wheelset yaw and its application in wheel wear prediction," *Wear*, vol. 432–433, 2019, doi: 10.1016/j.wear.2019.202958.

[6] H. Magalhaes *et al.*, "Wheel-rail contact models in the presence of switches and crossings," *Veh. Syst. Dyn.*, pp. 1–33, Mar. 2022, doi: 10.1080/00423114.2022.2045026.

[7] H. Magalhães *et al.*, "Implementation of a non-Hertzian contact model for railway dynamic application," *Multibody Syst. Dyn.*, vol. 48, no. 1, pp. 41–78, Jan. 2020, doi: 10.1007/s11044-019-09688-y.

[8] F. Marques, H. Magalhães, J. Pombo, J. Ambrósio, and P. Flores, "A three-dimensional approach for contact detection between realistic wheel and rail surfaces for improved railway dynamic analysis," *Mech. Mach. Theory*, vol. 149, p. 103825, Jul. 2020, doi: 10.1016/j.mechmachtheory.2020.103825.

[9] F. Marques et al., "On the generation of enhanced lookup tables for wheel-rail contact models," Wear, vol. 434–435, p. 202993, Sep. 2019, doi: 10.1016/j.wear.2019.202993.